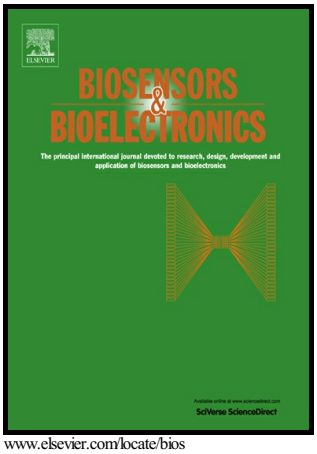

www.elsevier.com/locate/bios

Monitoring *in vivo* Metabolic Flux with a Designed Whole-cell Metabolite Biosensor of Shikimic Acid

Heng Li, Chaoning Liang, Wei Chen, Jian-Ming Jin, Shuang-Yan Tang, Yong Tao

PII: S0956-5663(17)30470-0
DOI: http://dx.doi.org/10.1016/j.bios.2017.07.022
Reference: BIOS9855

To appear in: *Biosensors and Bioelectronic*

Received date: 10 March 2017
Revised date: 1 June 2017
Accepted date: 8 July 2017

Cite this article as: Heng Li, Chaoning Liang, Wei Chen, Jian-Ming Jin, Shuang Yan Tang and Yong Tao, Monitoring *in vivo* Metabolic Flux with a Designe Whole-cell Metabolite Biosensor of Shikimic Acid, *Biosensors an Bioelectronic,* http://dx.doi.org/10.1016/j.bios.2017.07.022

Monitoring in vivo Metabolic Flux with a Designed Whole-cell Metabolite Biosensor of Shikimic Acid

Heng Li[a,c1], Chaoning Liang[a1], Wei Chen[a], Jian-Ming Jin[b*], Shuang-Yan Tang[a*], Yong Tao[a]

[1]CAS Key Laboratory of Microbial Physiological and Metabolic Engineering, Institute of Microbiology, Chinese Academy of Sciences, Beijing 100101, China

[2]Beijing Key Laboratory of Plant Resources Research and Development, Beijing Technology and Business University, Beijing 100048, China

[3]University of Chinese Academy of Sciences, Beijing 100049, China

jinjianming@btbu.edu.cn
tangsy@im.ac.cn

[*]Corresponding author

ABSTRACT

Knowledge of intracellular metabolite levels is important for the understanding of metabolic flux distributions. Whole-cell biosensors of key metabolites are ideal for the monitoring of carbon flow in important metabolic pathways, thus guiding metabolic engineering for microbial improvement. However, lack of biosensors for metabolites of interests has limited their applications. In this study, a genetically encoded whole-cell biosensor specifically responding to shikimic acid has been developed by screening a site-saturation mutagenesis library of the

[1] These authors contributed equally to the work.

binding pocket of a uric acid-responsive regulatory protein. This biosensor has been successfully applied in analyzing and engineering metabolic flux in the shikimic acid pathway, through genome-wide screening of gene targets critical for the pathway flux, and by improving the specific activity of pathway key enzyme, AroG. This work demonstrates the feasibility of monitoring metabolic flux with the aid of whole-cell biosensors designed for key metabolites.

Keywords: Whole-cell biosensor; High-throughput screening; Metabolic flux; Regulatory protein; Shikimic acid

1. Introduction

Key metabolite levels reflect the overall cellular metabolic state. Sensitive whole-cell biosensors of key metabolites allow real-time monitoring of the carbon flow in metabolic pathways (Rogers and Church, 2016; Rogers et al., 2015; Zhangand Keasling, 2011). This approach is much more rapid and simple than the classical isotopic or mass spectrometric determination methods (Albermann et al., 2011; Choi and Antoniewicz, 2011; Tang et al., 2009; Young et al., 2014). In addition to their use in metabolic flux analyses, whole-cell biosensors of key metabolites may also be applied in metabolic flux engineering as high-throughput screening tools.

Various genetic components can be adapted for the construction of whole-cell biosensors. Enzymes have been used in the development of such sensors, e.g.,

ATP sensor (Llaudet et al., 2005). Fluorescence resonance energy transfer (FRET) biosensors that take advantage of small molecule-induced FRET to evaluate the intracellular concentrations of target molecules consist of a specific effector binding domain with fluorescent proteins that function as FRET donor and acceptor fused at its ends (Frommer et al., 2009)(e.g., FRET biosensors for NADH (Zhao et al., 2011)). Further, transcriptional factors that respond to cellular metabolites to fine-regulate physiological activity of the cell can be successfully adapted in whole-cell metabolite biosensors (Rogersand Church, 2016; Rogers et al., 2015; Zhang and Keasling, 2011). For example, regulatory protein FadR responsive to acyl-CoA, have been employed for a dynamic control of biosynthetic pathways (Zhang et al., 2012). However, innate transcription factors that would be responsive to many target metabolites are still unavailable.

Shikimic acid pathway is present in microorganisms and plants, where it is used for the biosynthesis of L-phenylalanine, L-tyrosine, and L-tryptophan (Herrmannand Weaver, 1999). Metabolic engineering strategies that enhance the metabolic flux in shikimic acid pathway have been reported, these are relatively numerous because of this pathway's significance in the biosynthesis of aromatic amino acids and derived aromatic compounds such as flavonoids, stilbene, coumarin, and so on (Gosset, 2009; Kramer et al., 2003; Rodriguez et al., 2014).

Shikimic acid pathway starts with the condensation of phosphoenolpyruvate (PEP) and D-erythrose 4-phosphate (E4P) to 3-deoxy-D-arabino-heptulosonate-7-phosphate (DAHP) (Herrmann and Weaver, 1999). This entrance reaction

comprises a committed step of the pathway. In Escherichia coli, this step is mediated by three different DAHP synthases, AroG, AroF, and AroH, which are feedback-inhibited by L-phenylalanine, L-tyrosine, and L-tryptophan, respectively (Lin et al., 2012; Sprenger, 2007). The enzyme AroG comprises ~80% of the total DAHP synthase activity and is significantly more resistant to specific proteolysis than other DAHP synthases (Lin et al., 2012). Mutagenesis studies aiming at eliminating the feedback inhibition of DAHP synthases have been published, e.g., resulting in the construction of a feedback-resistant variant $AroG^{fbr}$ (Hu et al., 2003). The feedback-resistant DAHP synthase is typically overexpressed in an engineered strain for an increased flux in the shikimic acid pathway (Rodriguez et al., 2014). Nevertheless, attempts to improve the catalytic activity of this essential enzyme are still few, partially due to the lack of an efficient screening method.

In the current study, we aimed to engineer effector specificity of a regulatory protein to develop a whole-cell genetically encoded biosensor that could be readily applied in metabolic flux monitoring. A whole-cell shikimic acid biosensor was developed based on a regulatory system responding to uric acid in E. coli (Fig. 1a). To test its effectiveness, the biosensor was applied in engineering a DAHP synthase with an elevated specific activity, as well as in genome-wide screening of target genes that influence the metabolic flux in shikimic acid pathway. Our work demonstrates the feasibility of developing whole-cell biosensors of key metabolites by altering the effector specificity of regulatory proteins and the effectiveness of these biosensors in monitoring flux in a metabolic pathway.

2. Materials and methods

2.1. General

Restriction enzymes were purchased from New England Biolabs (Beijing, China) and DNA polymerases were purchased from Takara Bio Inc. (Dalian, China). T4 DNA ligase was purchased from Life Technologies (Shanghai, China). Oligonucleotides were synthesized by Life Technologies (Shanghai, China). Shikimic acid, PEP and E4P were purchased from Sigma-Aldrich (St. Louis, USA).

All bacteria were routinely grown in Luria-Bertani (LB) medium. The antibiotics ampicillin (100 μg·mL^{-1}), kanamycin (50 μg·mL^{-1}) and chloramphenicol (25 μg·mL^{-1}) were used when necessary.

2.2. Plasmid construction

All plasmids and primers used in this study are listed in Table S1 and S2, respectively. Standard manipulation was carried out for polymerase chain reaction (PCR), DNA purification, enzyme digestion, and DNA ligation.

1) pSH. The plasmid pSH was derived from plasmid pSHYa (Liang et al., 2015). The PCR product was amplified using primers SH-SacI-fwd and SH-SacI-rev with plasmid pSHYa as template, and then it was self-ligated after digestion with SacI, resulting in plasmid pSH.

2) pAroG^{fbr}. The gene aroG was amplified using the genomic DNA of E. coli MG1655 as template with primers aroG-EcoRI-fwd and aroG-PstI-rev. The PCR products were ligated into vector pSM04 (Chen et al., 2015) after digestion with EcoRI and PstI, and the kan gene (kanamycin resistance marker) from pSM04 was next replaced with the cat gene expressing chloramphenicol resistance, resulting in plasmid pAroG. Mutation L175D were introduced into aroG gene using a Stratagene QuikChange Site-Directed Mutagenesis Kit (Agilent Technologies Inc, Santa Clara, USA), using primers aroG-L175D-fwd and aroG-L175D-rev, resulting in plasmid pAroG^{fbr}.

3) pET28a-AroG^{fbr}. The aroG^{fbr} gene from plasmid pAroG^{fbr} was amplified using primers aroG-pET-NheI-fwd and aroG-pET-EcoRI-rev. The PCR product was ligated into pET28a after digestion with NheI and EcoRI, resulting in plasmid pET28a-AroG^{fbr}.

4) pTn10. Fragment F1 containing genes tnp* encoding Tn10 transposase (Genbank accession No. AF310136) under the control of P_{tac} promoter, and mob encoding Mob protein (Genbank accession No. NZ_LSAZ01000024) was synthesized by GENEWIZ (Suzhou, China) (Table S3). After digestion with XbaI and XhoI, fragment F1 was ligated into the PCR product amplified with primers GEX-XhoI-fwd and GEX-XbaI-rev using plasmid pGEX-6P-1 (GE Healthcare) as template, resulting in plasmid pGEX-TM. Fragment F2 containing R6K replication origin was amplified with primers R6K-NotI-fwd and R6K-overlap-rev using plasmid pAH156 (Haldimann and Wanner, 2001) (Genbank accession No.

AY048737) as template. Fragment F3 containing IS10R (left), gene kan, and IS10R (right) was amplified using plasmid pSM04 (Chen et al., 2015) as template with primers IS-overlap-fwd and IS-SacII-rev. Fragment F2 and F3 were PCR-assembled with primers R6K-NotI-fwd and IS-SacII-rev, resulting in fragment F4. After digestion with NotI and SacII, fragment F4 was ligated into the PCR product amplified with primers lacI-SacII-fwd and amp-NotI-rev using plasmid pGEX-TM as template, resulting in plasmid pTn10.

2.3. Strain construction

All strains used in this study are listed in Table S1. The aroA gene in strain E. coli DH5α was deleted via the one-step inactivation method as described (Datsenko and Wanner, 2000). Primers ΔaroA-fwd and ΔaroA-rev were used to delete gene aroA in strain DH5α, resulting in strain SA1. The primer sets, ΔsucA-fwd/ΔsucA -rev, Δagp-fwd/Δagp-rev, ΔnanS-fwd/ΔnanS -rev, ΔpphB-fwd/ΔpphB-rev, Δgnd-fwd/Δgnd -rev, were used for the deletion of genes sucA, agp, nanS, pphB and gnd in strain SA3, resulting in strains SA3-ΔsucA, SA3-Δagp, SA3-ΔnanS, SA3-ΔpphB and SA3-Δgnd, respectively. Plasmid pKD13 was used as template to obtain PCR products, which were purified, treated with DpnI and then used to transform the target strains carrying Red helper plasmid pKD46. Kanamycin resistant colonies were isolated, and the deletion was verified by PCR. The FRT-flanked kan gene was then eliminated using flipase-mediated recombination.

Strain SA3 was constructed by transformation of strain SA1 with pAroG^{fbr}.

To construct strain SA4, the fragment containing gene encoding the SH4 mutant and the P_{hucR}-RFP construct was amplified with primers SH-SacII-fwd and SH-XhoI-rev, using plasmid pSH as template. This fragment was ligated into the PCR product amplified using primers pAH156-XhoI-fwd and pAH156-SacII-rev with the CRIM plasmid pAH156 (Haldimann and Wanner, 2001) as template after digestion with XhoI and SacII, resulting in a construct in which the fragment was adjacent to the gentamycin resistance gene and flanked by regions homologous to the E. coli HK022 integration site. The fragment was integrated into the chromosome of strain SA1 using helper plasmid pAH69 as described (Haldimann and Wanner, 2001), resulting in strain SA4. The integration was verified by PCR.

2.4. Construction of HucR library

Overlap extension PCR was performed for the construction of site-saturation mutagenesis library of HucR. Two parallel PCR were performed to amplify two hucR gene segments using the following two sets of primers: hucR-lib-W20-fwd/ hucR-lib-L44-overlap-rev and hucR-lib-L44-overlap-fwd/hucR-lib-D73R80-rev. Equimolar aliquots of the two amplified fragments (1.6 nmole each) were PCR-assembled. The PCR product was used as mega-primer to perform mega-primer PCR of whole plasmid (MEGAWHOP PCR) (Miyazaki, 2003) using plasmid pSH as template. Following the MEGAWHOP PCR, DpnI digestion (20 U) was performed at 37^{o}C for 12 h, then DpnI was inactivated at 80^{o}C for 20 min.

The PCR products were use to transform E. coli MC1061 and around 2×10^6 transformants were recovered. Ten randomly picked clones were sequenced, revealing the expected random mutations at the targeted nucleotide positions (corresponding to site saturation at residue positions 20, 44, 73 and 80), with no additional point mutations. All colonies from the agar plates were used for plasmid isolation to prepare the plasmid library.

2.5. Screening of HucR library

The HucR plasmid library was used to transform strain DH5α (over 10^7 transformants were recovered). Fluorescence-activated cell sorting (FACS) was performed on a BD FACS Aria III flow cytometer (BD Biosciences, San Jose, USA). Fluorescence was excited at 561 nm, and emission was collected using a 610/20 nm band-pass filter. The library showed no fluorescence variation with the addition of shikimic acid (Fig. S1a). In the first round of negative screening, cells were precultured overnight in LB medium and then diluted to OD_{600}=0.2 in the same medium in the absence of inducer. The cells were then grown for 12 h and the least fluorescent 1.6×10^6 cells were collected from a total of 2×10^6 cells (representing 80% of all cells sorted). This was performed to eliminate HucR variants with high levels of leaky expression. The collected cells were then re-cultured in LB medium. 20 mM shikimic acid was added when OD_{600} reached 0.5, and the cells were further grown at 37°C for 5 h to enable positive screening. The most fluorescent 2×10^4 cells were sorted from a total of 2×10^6 cells. This

procedure was repeated in a second round of negative and positive screens. MOPS buffer (16 mM) was used to maintain pH around 7.0 in all the culturing. This dual screening was repeated seven times, followed by a final round of negative screening in the absence of inducer. The library showed increased fluorescence in the presence of shikimic acid after screening (Fig. S1b). Eight clones were selected for rescreening in test tubes in the presence of 20 mM shikimic acid.

2.6. Construction and screening of transposon library

Strain SA3 harboring plasmid pSH carrying gene encoding the SH4 mutant was transformed with plasmid pTn10, and then plated on LB agar containing 1 mM IPTG. After incubation at 37°C for 16 h, the colonies with the highest RFP fluorescence were selected and re-inoculated on LB agar, together with wild-type strain. Again the colonies showing higher fluorescence than the wild-type strain were selected and cultured in 3 mL LB for RFP determination and shikimic acid quantification using HPLC.

To identify the location of the transposon insertion in the chromosome, the thermal asymetric interlaced (TAIL)-PCR was conducted as described (Liu and Whittier, 1995; Sessions et al., 2002). Strains exhibiting increased shikimic acid productions were cultured and harvested to isolate genomic DNA. 100 ng of the genomic DNA was used as template for TAIL-PCR. Genomic sequences flanking the transposon were amplified with a mixture of four arbitrary degenerate (AD) primers (AD1-4), plus the specific primer inside the kan gene, kan-SP1, kan-SP2

and kan-SP3, individually. Three rounds of TAIL-PCR cycling were performed. The tertiary TAIL-PCR product was purified and sequenced using primer sp-seq. The sequence obtained was blasted in the database of E. coli K-12 strain MG1655 (http://ecocyc.org/) to identify the location of the transposon insertion in the chromosome. The location was further verified using PCR with primers kan-SP3 plus the primer designed according to the chromosome DNA sequence close to the insertion point.

2.7. Construction and screening of AroG^{fbr}random mutagenesis library

The random mutagenesis library of AroG^{fbr} was constructed through error-prone PCR. Primers aroG-EcoRI-fwd and aroG-PstI-rev were used to amplify aroG^{fbr}, using plasmid pAroG^{fbr} as template. The PCR reaction mixture consisted of 5 mM $MgCl_2$, 0.2 mM each of dATP and dGTP, 1 mM each of dCTP and dTTP, 0.05 mM $MnCl_2$ and rTaq DNA polymerase. Then the PCR products obtained, containing randomly mutated aroG^{fbr} gene, was used as the megaprimer to perform the MEGAWHOP PCR using pAroG^{fbr} as template. Following the MEGAWHOP PCR, DpnI digestion (20 U) of the template was performed at 37°C for 5 h, then DpnI was inactivated at 80°C for 20 min. The PCR products were used to transform E. coli MC1061 and around 1×10^5 transformants were recovered. Ten randomly picked clones from the library were sequenced and contained an average of 3 nucleotide mutations per clone. All colonies from the agar plates were used for plasmid isolation to prepare the plasmid library.

The random mutagenesis library was used to transform strain SA4. Cells were plated on LB agar containing10 μM IPTG. The screening was done as described above.

2.8. RFP expression fluorescence assay

A colony of strain DH5α harboring plasmid pSH were grown for 12 h in LB medium, then diluted to OD_{600}= 0.01 in the same medium containing an appropriate concentration of shikimic acid, and allowed to grow under inducing condition for 5 h. A total of 500 μL of culture was centrifuged, and the cells were washed with 100 mM potassium phosphate buffer (pH 7.0) and resuspended in 500 μL of the same buffer. The cell density (OD_{600}) and fluorescence emission was measured with a SynergyMx Multi-Mode Microplate Reader (BioTek, Vermont, USA)(556 nm excitation filter and 586/20 nm emission filter). The background fluorescence due to buffer was subtracted in all measurements, and the fluorescence data were normalized with respect to OD_{600}. OD_{600} of all the samples was around 1.8-2.0. The induction fold was calculated as the ratio of fluorescence of fully induced cells over fluorescence of non-induced cells.

A colony of strain SA3 harboring plasmid pSH carrying gene encoding the SH4 mutant, or strain SA4 harboring plasmid $pAroG^{fbr}$, was grown for 12 h in LB medium, then diluted to OD_{600}= 0.01 in the same medium containing 10 μM IPTG, and allowed to grow for 12 h. The RFP fluorescence of the culture was measured as described above.

2.9. Purification of 6-His tagged AroG^{fbr} and its mutants

A single colony of strain E. coli BL21 (DE3) harboring plasmid pET28a-AroG^{fbr} was grown in 3 mL of LB at 37^{o}C for 12 h. The culture was then diluted to OD_{600}=0.01 and grown at 37^{o}C, and 0.5 mM IPTG was added when OD_{600} reached 0.8, then the culture was continuously grown at 30^{o}C for 24 h. Cells were harvested by centrifugation at 4^{o}C at 3,000 ×g for 10 min. The cells were then resuspended in 50 mM Tris-HCl buffer (pH 7.5) and lysed by sonication with a JY92-IIN Ultra Sonic Cell Crusher (Ningbo, China). The lysate was centrifuged at 15,000 ×g for 30 min at 4^{o}C and the supernatant was applied to Ni-NTA resin (Sigma-Aldrich, St. Louis, USA). The column was washed with washing buffer (50 mM Tris–HCl, 300 mM NaCl, 20 mM imidazole, pH8.0) and the bound protein was eluted with elution buffer (50 mM Tris-HCl, 300 mM NaCl, 250 mM imidazole, pH 8.0). Imidazole was removed by dialysis at 4^{o}C against 50 mM Bis-Tris propane buffer (pH 6.8, 10 μM EDTA). The purity of proteins were assessed by sodium dodecyl sulfate polyacrylamide gel electrophoresis (SDS-PAGE) and the protein concentration was assayed with Bradford method (Bradford, 1976).

2.10. HPLC quantification of shikimic acid

The cell culture was centrifuged at 12,000 ×g for 5 min, and the supernatant was filtrated through a 0.22 μm filter and analyzed with HPLC. A Shimadzu LC-20A HPLC system (Shimadzu Corp., Kyoto, Japan) equipped with a SPD-M20A photodiode array (PDA) detector operating at 210 nm was used for the quantification. Separation of products was achieved using a Bio-Rad Aminex HPX-87H Column (10 μm, 7.8×300 mm, Bio-Rad, Hercules, USA) operating at 50°C. The mobile phase was 5 mM H_2SO_4 with a flow rate of 0.45 mL/min. The retention time of shikimic acid was 15.7 min. The shikimic acid concentrations were calculated using a standard curve prepared using authentic shikimic acid.

2.11. Activity assay for $AroG^{fbr}$

$AroG^{fbr}$ activity was assayed as described by Schoner and Herrmann (Schoner and Herrmann, 1976), based on the absorbance difference at 232 nm between PEP (ε=2800) and DAHP (ε=415). A mixture containing appropriate concentrations of PEP and E4P in 1 mL of 0.01 M Bis-Tris propane buffer (pH 7.0) was pre-incubated at 25°C for 10 min. The reaction was started by addition of 1 μl of the purified enzyme, The activity of $AroG^{fbr}$ was determined at 25^{o}C by monitoring the absorbance change at 232 nm with a SynergyMx Multi-Mode Microplate Reader. One unit of $AroG^{fbr}$ activity is defined as the amount of $AroG^{fbr}$ enzyme required to form 1 μmole of DAHP per minute.

2.12. Kinetic parameters determination

The kinetic parameters of $AroG^{fbr}$ were determined by Lineweaver–Burk plots. $AroG^{fbr}$ activity assay was performed as described above at different substrate concentrations (6.7-250 mM of PEP in the presence of 500 mM E4P or 67-200 mM of E4P in the presence of 500 mM PEP) for both $AroG^{fbr}$ parent and mutant enzymes. All reported data in Table 2 represent the mean of three independent data points.

3. Results

3.1. Designing a whole-cell biosensor of shikimic acid by engineering the HucR regulatory protein

Uric acid regulatory system from Deinococcus radiodurans has been adapted in E. coli (Liang et al., 2015). Briefly, in this system, RFP expression from promoter P_{hucR} is repressed by HucR regulatory protein, the binding of uric acid to HucR induces a conformational change within this protein, resulting in the release of the promoter DNA from HucR and activation of the transcription from promoter P_{hucR} (Wilkinson and Grove, 2004; Wilkinson and Grove, 2005). To engineer the effector specificity of HucR, an HucR library containing a simultaneous site saturation mutagenesis of four amino acid positions located in the HucR effector binding pocket (W20, L44, D73 and R80) (Bordelon et al., 2006), was constructed. After transforming E. coli DH5α, the transformants were screened by fluorescence-activated cell sorting (FACS) to collect HucR variants responding to exogenous 20 mM shikimic acid ("positive" screening). Variants with high levels

of leaky expression were eliminated by collecting the least fluorescent cells in the absence of shikimic acid ("negative" screening). After seven rounds of positive/negative sorting, eight HucR variants responsive to shikimic acid were identified, among which mutant SH4 (W20C, L44F, D73T, R80A) displays the strongest response to shikimic acid (Fig.1b, Fig. S1c). Fig.1c depicts RFP fluorescence of E. coli DH5α strain expressing the mutant protein SH4, as a function of shikimic acid concentration. An ~18-fold induction of RFP expression was achieved over a shikimic acid concentration range of 0-20 mM, with half-maximal induction occurring in the presence of~6.2 mM shikimic acid. The wild-type HucR protein did not respond to shikimic acid at all (Fig. 1c). The inducing effect of a series of shikimic acid analogs, including gallic, cinnamic, caffeic, and quinic acids, as well as the natural inducer of HucR, uric acid, on SH4 mutant was assessed (Fig. 1d). The induction of SH4-controlled RFP expression was much higher in response to shikimic acid than to the other compounds tested, revealing good induction specificity of the SH4 mutant. To test the applicability of the cell expressing the SH4 mutant as a whole-cell shikimic acid biosensor for reporting the carbon flow in the shikimic acid pathway in vivo, E. coli strain DH5α expressing the SH4 mutant was transformed with plasmid pAroG^{fbr} carrying gene encoding the feedback-resistant variant of the DAHP synthase AroG. The RFP fluorescence of the strain expressing AroG^{fbr} was pronouncedly enhanced compared with that of the control strain without the aroG^{fbr} gene (Fig. 1e). This

indicated that the developed whole-cell shikimic acid biosensor could effectively report intracellular flux in the shikimic acid pathway.

For high-quality biosensors, specificity, sensitivity and robustness are all important features. Due to the complicated intracellular environment, only the result showing that the output signal is proportional to the molecular concentration is not enough to validate the biosensor's effectiveness in practice. More metabolic engineering work using this whole-cell biosensor as a screening tool was done, to further demonstrate its functionality.

3.2. Shikimic acid levels in wild-type and engineered E. coli DH5α strains

The shikimic acid concentration was too low to be detected by HPLC in the wild-type E. coli DH5α strain cultured in LB medium for 12 h (data not shown). To obtain cells with intracellular shikimic acid concentrations detectable by HPLC, we knocked out aroA (strain SA1), the gene encoding 5-enol-pyruvylshikimate-3-phosphate (EPSP) synthase that catalyzes the transfer of the enolpyruvoyl moiety from PEP to the hydroxyl group of carbon 5 of shikimate-3-phosphate with the elimination of phosphate, to produce EPSP (Kishore et al., 1986). This led to the accumulation of shikimic acid since the downstream shikimic acid transformations were blocked. Alternatively, we overexpressed $AroG^{fbr}$ in E. coli DH5α to increase metabolic flux in the shikimic acid pathway (strain SA2). Nevertheless, shikimic acid was not detected in strain SA1, while its concentration in SA2 strain culture was 0.6 mg/L. Overexpressing $aroG^{fbr}$ in strain SA1(resulting in strain SA3) led to a further enhancement of shikimic acid accumulation (8.6

mg/L), and this strain was therefore used for further engineering experiments (Fig. 2a).

3.3. Development and validation of a high-throughput screening technique for shikimic acid

Shikimic acid pathway connects central carbon metabolism to the biosynthesis of chorismate (Bongaerts et al., 2001). Improving the metabolic flux in shikimic acid pathway would increase the biosynthesis of aromatic amino acids, as well as downstream aromatic compounds, many of which are widely used in pharmaceutical, food, healthcare, and cosmetics industries (Juminaga et al., 2012; Kang et al., 2012; Rodriguez et al., 2015a; Wu et al., 2013). Until now, a series of genes have been reported that affect the flux in shikimic acid pathway (Chandran et al., 2003; Cui et al., 2014; Rodriguez et al., 2015b). To rapidly identify the target genes whose inactivation leads to improved shikimic acid pathway flux on a whole-genome scale, a transposon insertion library was constructed in the strain SA3 bearing plasmid pSH carrying gene encoding the SH4 mutant. Gene disruptions influencing the metabolic flux in shikimic acid pathway would lead to the change of intracellular shikimic acid concentration, which could be monitored by assessing the SH4 mutant-controlled RFP expression. Thus, mutant strains with a high metabolic flux in the shikimic acid pathway could be easily selected by measuring cell fluorescence.

To validate the high-throughput screening technique, thirty clones were

randomly selected from the transposon library. They were cultured in liquid LB medium and the RFP fluorescence and shikimic acid titers were determined (Fig. 2b). The RFP fluorescence correlated well with cellular shikimic acid levels, thus indicating the effectiveness of the developed whole-cell shikimic acid biosensor as a high-throughput screening tool of intracellular shikimic acid concentrations.

3.4. Screening the transposon library for mutant strains with improved shikimic acid pathway flux

Ten clones were randomly selected from the transposon library and the locations of the transposon insertions were determined (Table S4). The data indicated that the locations of these insertions were random, and no obvious hotspots of transposon insertion were apparent. Further, eight clones with the highest RFP fluorescence were selected from~1×10^4 transformants screened from the library. They all produced higher quantities of shikimic acid than the starting strain (Fig. 3a). The location of the transposon insertion in each mutant was identified (Table 1 and Fig. 3b). Five target genes inactivated by the transposons (sucA, agp, nanS, pphB, gnd) were individually knocked out in strain SA3 and the enhanced shikimic acid formation was confirmed in the deletion mutant strains (Fig. S2).

3.5. Engineering of the DAHP synthase $AroG^{fbr}$

DAHP synthase has been widely studied because of the feedback, allosteric regulation of its activity by aromatic amino acids (Lin et al., 2014; Lin et al., 2012).

Improving its specific activity is essential for the construction of strains with high metabolic flux in the shikimic acid pathway. Since AroG is the main DAHP synthase in E. coli and the structural basis for its feedback inhibition by L-phenylalanine has been elucidated (Jiang et al., 2000), its feedback-resistant variant, $AroG^{fbr}$, was used as the parent enzyme in protein engineering experiments. To improve the $AroG^{fbr}$ activity, random mutagenesis library of $AroG^{fbr}$ was constructed and subjected to a directed evolution. The $AroG^{fbr}$ library was used to transform strain SA4 constructed by simultaneously integrating the constitutively-expressed gene encoding the SH4 mutant and the P_{hucR}-RFP construct into the chromosome of strain SA1. The library was screened as described above. Five mutant strains were selected from 3×10^4 transformants screened, and they were cultured in LB and their shikimic acid concentrations were determined by HPLC. They produced more shikimic acid than the strain expressing the parental $AroG^{fbr}$, with mutants M2 and M3 producing 2.6 and 2.2 times more shikimic acid, respectively, than the parental strain (Fig. 4a). The plasmids were isolated from these strains and used to individually retransform strain SA4, and elevated RFP expression and shikimic acid production was confirmed in the transformants. Sequencing revealed amino acid substitutions in the mutated enzymes (Table 2).

3.6. Kinetic analysis of the mutated $AroG^{fbr}$ proteins

To further investigate the kinetic properties of mutated AroG^{fbr} proteins produced by shikimic acid hyper-producers selected from the library, the mutated aroG^{fbr} genes were re-cloned into vector pET28a and N-terminal His-tagged enzymes were purified. The specific activities of the parental and mutant enzymes were all higher at higher E4P concentrations, due to their poorer affinity for the E4P substrate (Fig. 4b). All mutants had higher specific activities than the parental AroG^{fbr}. In the presence of high PEP and low E4P concentrations, the specific activities of M1 and M2 were ~1.4 and 1.9-fold higher, respectively, than that of the parental enzyme, because of their improved affinity for and catalytic efficiency toward E4P. In contrast, mutant M3 showed the highest specific activity in the presence of low PEP and high E4P concentrations. Since the endogenous E4P levels are relatively low compared with PEP (Toya et al., 2010), M2 mutant produced the highest concentrations of shikimic acid.

Kinetic analyses of the parental and mutant AroG^{fbr} proteins were performed (Table 2). The kinetic investigation revealed that, compared with the parent, affinities of the three mutants for PEP were all reduced, resulting in decreased catalytic efficiencies, except for M3, which was characterized by an obviously increased k_{cat} value.The affinities of mutant M1 and M2 for the E4P substrate were obviously higher than that of parental AroG^{fbr}, leading to their significantly elevated catalytic efficiencies with E4P. The improved shikimic acid productions of strains expressing these mutant enzymes were in accordance with the measured catalytic efficiencies of these enzymes on E4P vs. PEP, indicating that the

intracellular E4P concentration is the limiting factor of metabolic flux in the shikimic acid pathway, and that improving the catalytic efficiency of AroG in the presence of E4P is critical for enhancing metabolic flux in this pathway. Feedback resistance of the $AroG^{fbr}$ mutants was evaluated. Mutants M1, M2, and M3 retained 91%, 86%, and 85% of enzymatic activity, respectively, in the presence of 1 mM L-phenylalanine, compared with 86% for the parental $AroG^{fbr}$. Thus, the mutant enzymes retained the original feedback resistance to L-phenylalanine.

4. Discussion

The primary goal of metabolic engineering is to design strains to achieve higher efficiencies in metabolite overproduction through alterations in metabolic flux distribution (Varma et al., 1994). A rapid and simple evaluation of flux in a metabolic pathway becomes essentially important in metabolic flux engineering. Intracellular levels of key metabolites are good markers of metabolic flux. However, the majority of metabolites are not easily translated into colorimetric or fluorescent outputs. Church group (Rogers and Church, 2016) used genetically encoded biosensors derived from transcription factors that were responsive to small molecules to obtain a fluorescent readout that would be proportional to the intracellular concentration of target metabolite. However, the lack of available transcription factors that respond to the metabolites of interest has hindered the applications of this kind of elegant biosensors. To facilitate more extensive applications of transcription factor-based small-molecule biosensors, in this study,

we aimed to demonstrate the feasibility of engineering the effector specificity of regulatory proteins to develop a genetically encoded whole-cell biosensors of key metabolites. A whole-cell biosensor of shikimic acid was developed by altering the induction specificity of regulatory protein HucR, from uric acid to shikimic acid. Using this novel biosensor, metabolic flux of shikimic acid pathway could be efficiently monitored.

Some genes within the metabolic network have been identified by rational design as important for the flux in shikimic acid pathway; however, a high-throughput genome-wide screen for genes that affect flux distribution of the shikimic acid pathway has not been attempted before because of the lack of screening tools. The whole-cell shikimic acid biosensor developed in this study was used to screen a library in E. coli cells for elevated shikimic acid concentrations. Some hits closely associated with the flux in shikimic acid pathway that had not been reported before were identified, demonstrating the effectiveness of the whole-cell shikimic acid biosensor which allows for the identification of gene targets that traditional metabolic engineering is unable to discover.

Among the gene targets identified, ptsH and bglF encode components of the PEP-dependent phosphotransferase system (PTS) (Fig. 3b). PTS consumes 50% of the available PEP (Escalante et al., 2012; Gosset, 2005). It has been reported that replacement of the PEP:carbohydrate phosphotransferase system with other transport systems, e.g., galactosepermease and glucokinase, significantly reduced

the consumption of PEP and improved shikimic acid production in E. coli (Balderas-Hernandez et al., 2009; Flores et al., 1996). Besides, PEP is also the substrate of NanS, which catalyzes the condensation of PEP and N-acyl-D-mannosamine-6-phosphate to form N-acylneuraminate-9-phosphate (Tsai, et al., 2011)(Fig. 3b).The disruption of gnd gene, which encodes 6-phosphogluconate dehydrogenase, led to a 185.7% increase of shikimic acid concentration (Fig. 3b), probably due to the improved metabolic flux in the glycolysis pathway resulting from the pentose phosphate pathway truncation, which led to increased levels of shikimic acid pathway substrates (Fig. 3b). Similarly, inactivation of sdhCDAB-sucABCD operon or agp gene (Fig. 3b) as well reduced the metabolic fluxes of the branch or downstream pathways of the glycolysis pathway.

Another application of the whole-cell biosensor is to engineer the first rate-limiting enzyme of the shikimic acid pathway. The improvement of AroG is of great significance, since using an improved key enzyme is much more advantageous than simply overexpressing it, when generating high-performance cells with low metabolic burden. Characterization of the AroG variants obtained in the study indicated that the poor catalytic capacity of the enzyme with respect to the E4P substrate is the main factor limiting the improvement of flux in the shikimic acid pathway. Here, using directed in vivo evolution coupled with high-throughput screening with the shikimic acid whole-cell biosensor, AroG variants with improved affinity for E4P were easily selected. Our study thus

revealed the advantage of in vivo directed evolution strategy for metabolic pathway enzyme engineering over rational design, since mutant enzymes overcoming a specific in vivo limitation could be selected.

5. Conclusions

A simple, rapid and reliable method to analyze intracellular metabolic flux is of important significance. Key metabolite levels reflect the overall cellular metabolic flux distributions. Compared with the widely-used isotopic or mass spectrometric determination methods, the whole-cell biosensors of key metabolites allows rapid monitoring of the intracellular metabolite levels simply by measuring cell fluorescence. The whole-cell biosensor of shikimic acid developed in this study has been demonstrated highly effective in optimizing the host chromosome or pathway key enzyme for improved metabolic flux of the shikimic acid pathway. The method described here should be potentially applicable to the design and application of whole-cell biosensors for various metabolites.

Acknowledgments

This work was supported by Ministry of Science and Technology of China Grant 2013CB734003, the National Natural Science Foundation of China (Grant No. 21472234, 31500054 and 31501037) and the CAS/SAFEA International Partnership Program for Creative Research Teams.

References

Albermann, C., Ghanegaonkar S., Lemuth K., Vallon T., Reuss M., Armbruster W., Sprenger G.A., 2008. Chembiochem 9, 2524-2533.
Balderas-Hernandez, V.E., Sabido-Ramos A., Silva P., Cabrera-Valladares N., Hernandez-Chavez G., Baez-Viveros J.L., Martinez A., Bolivar F., Gosset G., 2009. Microb. Cell Fact. 8, 19.
Bongaerts, J., Kramer M., Muller U., Raeven L., Wubbolts M., 2001. Metab. Eng. 3, 289-300.
Bordelon, T., Wilkinson S.P., Grove A., Newcomer M.E., 2006. J. Mol. Biol. 360, 168-177.
Bradford, M.M., 1976. Anal. Biochem. 72, 248-254.
Chandran, S.S., Yi J., Draths K.M., von Daeniken R., Weber W., Frost J.W., 2003. Biotechnol. Progr. 19, 808-814.
Chen, W., Zhang S., Jiang P., Yao J., He Y., Chen L., Gui X., Dong Z., Tang S.Y., 2015. Metab. Eng. 30, 149-155.
Choi, J., Antoniewicz M.R., 2011. Metab. Eng. 13, 225-233.
Cui, Y.Y., Ling C., Zhang Y.Y., Huang J., Liu J.Z., 2014. Microb. Cell Fact. 13, 21.
Datsenko, K.A., Wanner B.L., 2000. Proc. Natl. Acad. Sci. USA 97, 6640-6645.
Escalante, A., Cervantes A.S., Gosset G., Bolivar F., 2012. Appl. Microbiol.Biot. 94, 1483-1494.
Flores, N., Xiao J., Berry A., Bolivar F., Valle F., 1996. Nat. Biotechnol. 14, 620-623.
Frommer, W.B., Davidson M.W., Campbell R.E., 2009. Chem. Soc. Rev. 38, 2833-2841.
Gosset, G., 2005. Microb. Cell Fact. 4, 14-24.
Gosset, G., 2009. Curr. Opin. Biotechnol. 20, 651-658.
Haldimann, A., Wanner B.L., 2001. J. Bacteriol. 183, 6384-6393.
Herrmann, K.M., Weaver L.M., 1999. Annu. Rev. Plant Physiol. Mol. Biol. 50, 473-503.
Hu, C.Y., Jiang P.H., Xu J.F., Wu Y.Q., Huang W.D., 2003. J. Basic Microbiol. 43, 399-406.
Jiang, P.H., Shi M., Qian Z.K., Li N.J., Huang W.D., 2000. Acta Biochim. Biophys. Sin. 32, 441-444.
Juminaga, D., Baidoo E.E.K., Redding-Johanson A.M., Batth T.S., Burd H., Mukhopadhyay A., Petzold C.J., Keasling J.D., 2012. Appl. Environ. Microb. 78, 89-98.
Kang, S.Y., Choi O., Lee J.K., Hwang B.Y., Uhm T.B., Hong Y.S., 2012. Microb. Cell Fact. 11, 153.
Kishore, G.M., Brundage L., Kolk K., Padgette S.R., Rochester D., Huynh Q.K., Dellacioppa G., 1986. Fed. Proc. 45, 1506-1506.
Kramer, M., Bongaerts J., Bovenberg R., Kremer S., Muller U., Orf S., Wubbolts M., Raeven L., 2003. Metab. Eng. 5, 277-283.

Liang, C.N., Xiong D.D., Zhang Y., Mu S.S., Tang S.Y., 2015. Appl. Microbiol. Biotech. 99, 2267-2275.
Lin, S.Y., Liang R., Meng X.J., OuYang H.S., Yan H.Y., Wang Y., Jones G.S., 2014. Int. J. Biol. Macromol. 68, 173-177.
Lin, S.Y., Meng X.J., Jiang J., Pang D.X., Jones G., OuYang H.S., Ren L.Z., 2012. Int. J. Biol. Macromol. 51, 915-919.
Liu, Y.G., Whittier R.F., 1995. Genomics. 25, 674-681.
Llaudet, E., Hatz S., Droniou M., Dale N., 2005. Anal. Chem. 77, 3267-3273.
Miyazaki, K., 2003. Methods in Mol. Biol. 231, 23-28.
Rodriguez, A., Kildegaard K.R., Li M., Borodina I., Nielsen J., 2015a. Metab. Eng. 31, 181-188.
Rodriguez, A., Kildegaard K.R., Li M.J., Borodina I., Nielsen J., 2015b. Metab. Eng. 31, 181-188.
Rodriguez, A., Martinez J.A., Flores N., Escalante A., Gosset G., Bolivar F., 2014. Microb. Cell Fact. 13, 126.
Rogers, J.K., Church G.M., 2016. Proc. Natl. Acad. Sci. U. S. A. 113, 2388-2393.
Rogers, J.K., Guzman C.D., Taylor N.D., Raman S., Anderson K., Church G.M., 2015. Nucleic Acids Res. 43, 7648-7660.
Schoner, R., Herrmann K.M., 1976. J. Biol. Chem. 251, 5440-5447.
Sessions, A., Burke E., Presting G., Aux G., McElver J., Patton D., Dietrich B., Ho P., Bacwaden J., Ko C., Clarke J.D., Cotton D., Bullis D., Snell J., Miguel T., Hutchison D., Kimmerly B., Mitzel T., Katagiri F., Glazebrook J., Law M., Goff S.A., 2002. Plant Cell. 14, 2985-2994.
Sprenger, G.A. 2007. Aromatic Amino Acids, in: Wendisch, V.F. (Eds.), Amino Acid Biosynthesis Pathways, Regulation and Metabolic Engineering. Springer, Heidelberg, pp. 93-127.
Tang, Y.J., Martin H.G., Myers S., Rodriguez S., Baidoo E.E., Keasling J.D., 2009. Mass Spectrom. Rev. 28, 362-375.
Toya, Y., Ishii N., Nakahigashi K., Hirasawa T., Soga T., Tomita M., Shimizu K., 2010. Biotechnol. Progr. 26, 975-992.
Tsai, S., Hardison N.E., James A.H., Motsinger-Reif A.A., Bischoff S.R., Thames B.H., Piedrahita J.A., 2011. Placenta. 32, 175-182.
Varma, A., Palsson B.O., Varma A., Palsson B.O., 1994. Nat. Biotechnol. 12, 994-998.
Wilkinson, S.P., Grove A., 2004. J. Biol. Chem. 279, 51442-51450.
Wilkinson, S.P., Grove A., 2005. J. Mol. Biol. 350, 617-630.
Wu, J.J., Liu P.R., Fan Y.M., Bao H., Du G.C., Zhou J.W., Chen J., 2013. J. Biotechnol. 167, 404-411.
Young, J.D., Allen D.K., Morgan J.A., 2014. Methods Mol. Biol. 1083, 85-108.
Zhang, F.Z., Carothers J.M., Keasling J.D., 2012. Nat. Biotechnol. 30, 354-U166.
Zhang, F.Z., Keasling J., 2011. Trends Microbiol. 19, 323-329.
Zhao, Y., Jin J., Hu Q., Zhou H.M., Yi J., Yu Z., Xu L., Wang X., Yang Y., Loscalzo J., 2011. Cell Metab. 14, 555-566.

Figure Captions:

Fig. 1. Development of the shikimic acid biosensor by engineering the HucR regulatory protein. (a) Schematic diagram of engineering of the HucR regulatory system responsive to shikimic acid in E. coli. (b) Eight clones were selected for re-screening after iterative FACS screening of strain library. They were all responsive to 20 mM shikimic acid. (c) RFP fluorescence of E. coli strain DH5α expressing the HucR mutant SH4, as a function of shikimic acid concentration. The corresponding dose-response curve of wild-type HucR is included for reference. (d) RFP fluorescence of E. coli strain DH5α expressing the HucR mutant SH4, in response to 10 mM of the indicated compounds. (e) RFP fluorescence of E. coli strain DH5α harboring plasmid pSH carrying gene encoding the HucR mutant SH4, with or without $AroG^{fbr}$ overexpression. The data are from three replicate experiments and are expressed as the mean±SD.

Fig. 2. Validation of the shikimic acid biosensor as a high-throughput screening tool. (a) Shikimic acid concentrations in wild-type and engineered E. coli DH5α strains, quantified by HPLC. (b) RFP fluorescence and shikimic acid concentrations in thirty clones randomly selected from the transposon library, compared with those of the wild-type strain SA3 harboring plasmid pSH carrying gene encoding the SH4 mutant. (c) Overview of the transposon library on LB agar supplemented with 10 μM IPTG. The selected clone with highest RFP fluorescence is marked with an arrow. The data are from three replicate

experiments and are expressed as the mean±SD.

Fig. 3. Genome-wide metabolic screening. (a) RFP fluorescence and shikimic acid concentrations of mutant strains selected from the transposon library. The data are from three replicate experiments and are expressed as the mean±SD. (b) Location of the transposon- inactivated genes (in red) in mutant strains selected from the transposon library in this study. Genes, whose inactivation (in green) or overexpression (in cyan) was reported before to lead to increased production of shikimic acid, are also presented. PTS, phosphotransferase system; G6P, glucose-6-phosphate; F6P, fructose-6-phosphate; G3P, glyceraldehyde-3-phosphate; 6PGNL, 6-phosphogluconolactone; 6PG, 6-phosphogluconate; Ru5P, ribulose-5-phosphate; R5P, ribose-5-phosphate; Xu5P, xylulose-5-phosphate; S7P, sedoheptulose-7-phosphate; E4P, erythrose-4-phosphate; PEP, phosphoenol-pyruvate; TCA, tricarboxylic acid cycle; NADM, N-acetyl-D-mannosamine; NA, N-acetylneuraminate; CoA, coenzyme A; DAHP, 3-deoxy-D-arabinoheptulosonate 7-phosphate; DHQ, 3-dehydroquinic acid; DHS, 3-dehydroshikimic acid; S3P, shikimic acid-3-phosphate; EPSP, 5-enolpyruvyl-shikimate-3-phosphate; CHA, chorismate.

Fig. 4. $AroG^{fbr}$ engineering. (a) The amount of shikimic acid produced by mutant strains selected from a library of randomly mutagenized $AroG^{fbr}$. (b) Specific activities of the parental and mutated $AroG^{fbr}$ enzymes in the presence of different

substrate concentrations. The data are from three replicate experiments and are expressed as the mean±SD.

Table 1 Genes where the transposon was inserted and percentage increase of shikimic acid production in the mutant strains selected from the transposon library compared with the parental strain.

Mutant strains	Genes where the transposon was inserted	Percentage increase of shikimic acid production
T1	sucC	136.6%
T10	agp	167.1%
T19	nanS	189.4%
T22	pphB	130.6%
T23	promoter of ptsH	208.5%
T26	bglF	175.4%
T27	promoter of sdhCDAB-sucABCD operon	168.0%
T39	gnd	185.7%

Table 2 Kinetic parameters of the parental and mutated $AroG^{fbr}$ enzymes for PEP and E4P substrates.

Enzymes	K_m (μM)		k_{cat} (s^{-1})	k_{cat}/K_m($s^{-1}\mu M^{-1}$)	
	PEP	E4P		PEP	E4P
$AroG^{fbr}$	25±0.3	120±8.5	119±3.5	4.8	1.0
M1：L179F	45±6.4	82±4.7	126±8.1	2.8	1.5
M2：K237R	44±1.4	72±4.1	205±2.6	4.7	2.8
M3：Y94H	53±4.0	348±30.3	384±10.6	7.2	1.1

Highlights

- A novel whole-cell biosensor specifically responsive to the key metabolite shikimic acid has been developed.
- With this whole-cell biosensor, the intracellular metabolic flux of shikimic acid pathway could be monitored by simply measuring the cell fluorescence.
- The whole-cell biosensor has been demonstrated effective in rapidly selecting beneficial mutant strains in engineering the metabolic network of the host strain to improve the shikimic acid pathway flux.

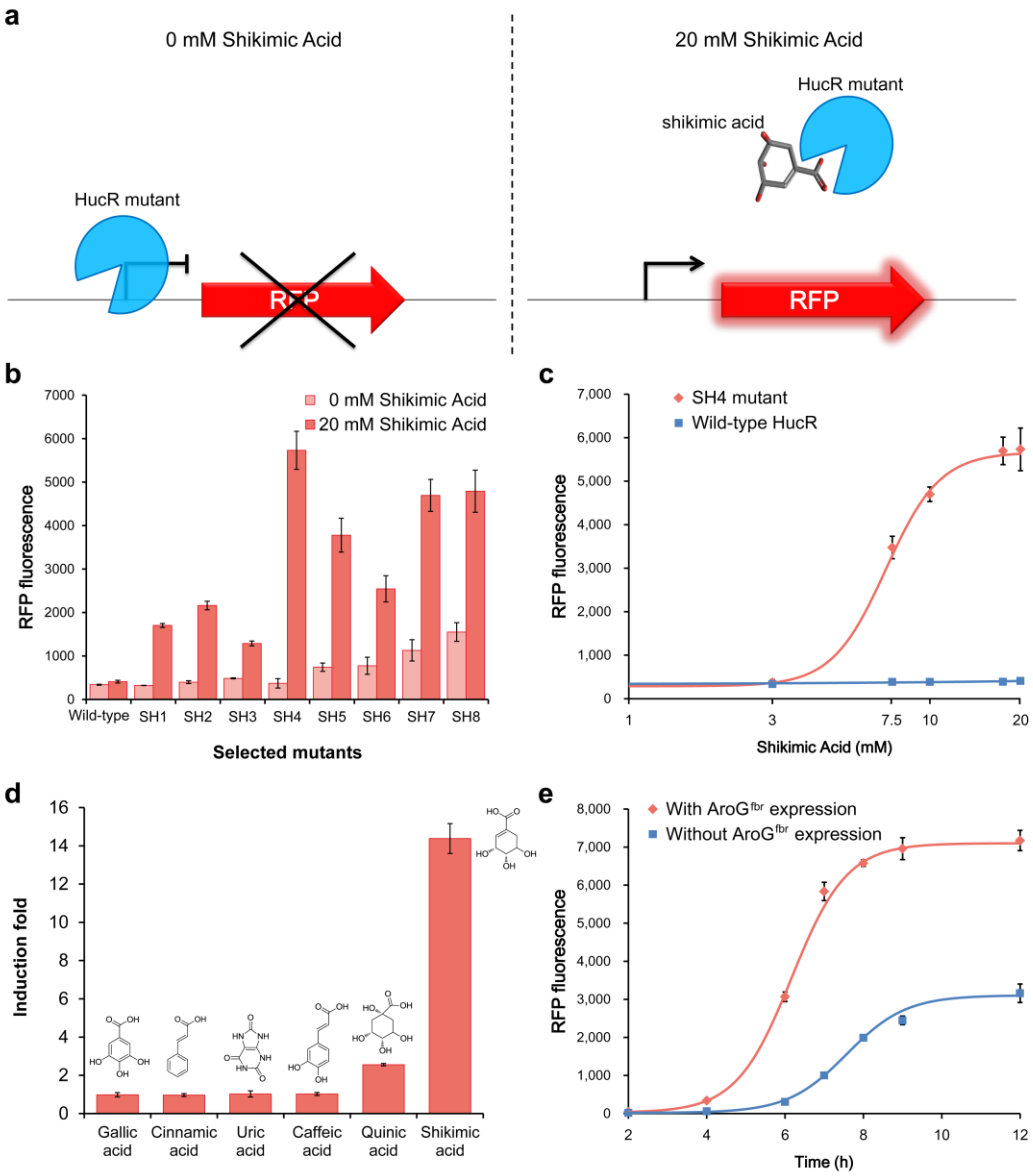
a
0 mM Shikimic Acid
20 mM Shikimic Acid
HucR mutant
shikimic acid
HucR mutant
RFP
RFP
b
0 mM Shikimic Acid
20 mM Shikimic Acid
RFP fluorescence
Wild-type SH1 SH2 SH3 SH4 SH5 SH6 SH7 SH8
Selected mutants
c
SH4 mutant
Wild-type HucR
RFP fluorescence
Shikimic Acid (mM)
d
Induction fold
Gallic acid
Cinnamic acid
Uric acid
Caffeic acid
Quinic acid
Shikimic acid
e
With AroG fbr expression
Without AroG fbr expression
RFP fluorescence
Time (h)

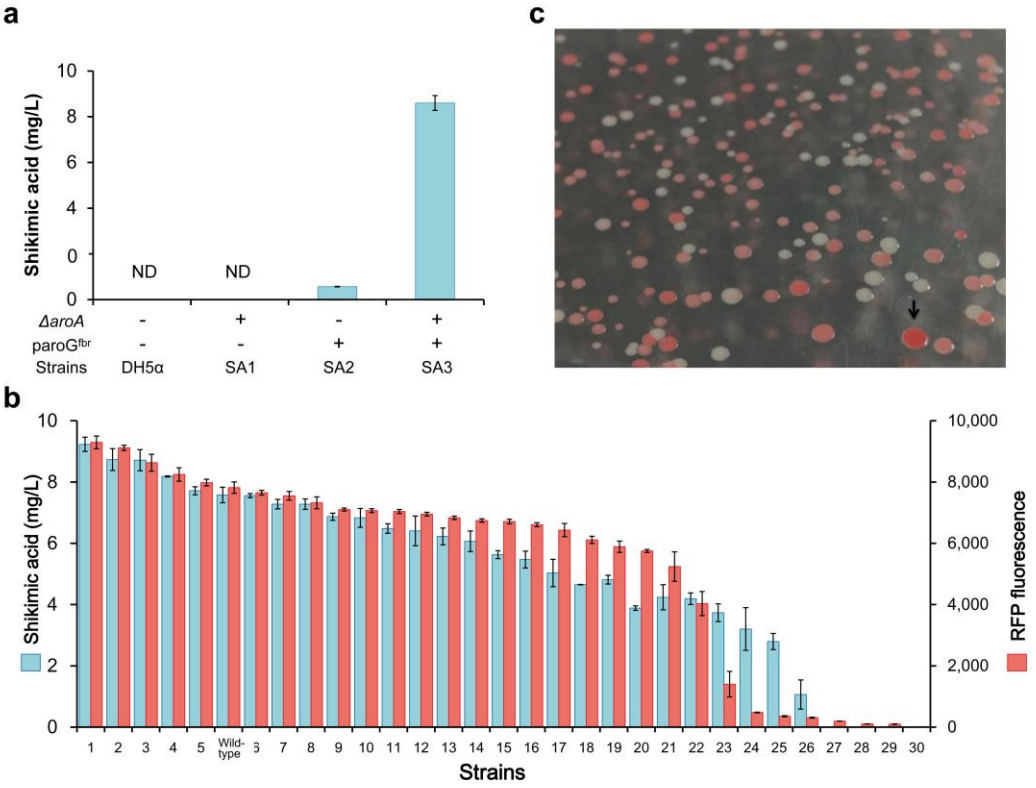

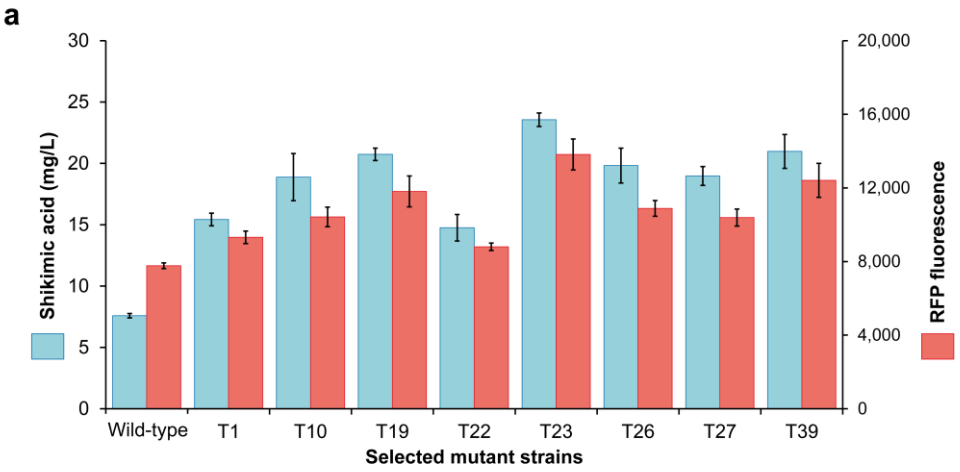
a
Shikimic acid (mg/L)
RFP fluorescence
Wild-type
T1
T10
T19
T22
T23
T26
T27
T39
Selected mutant strains

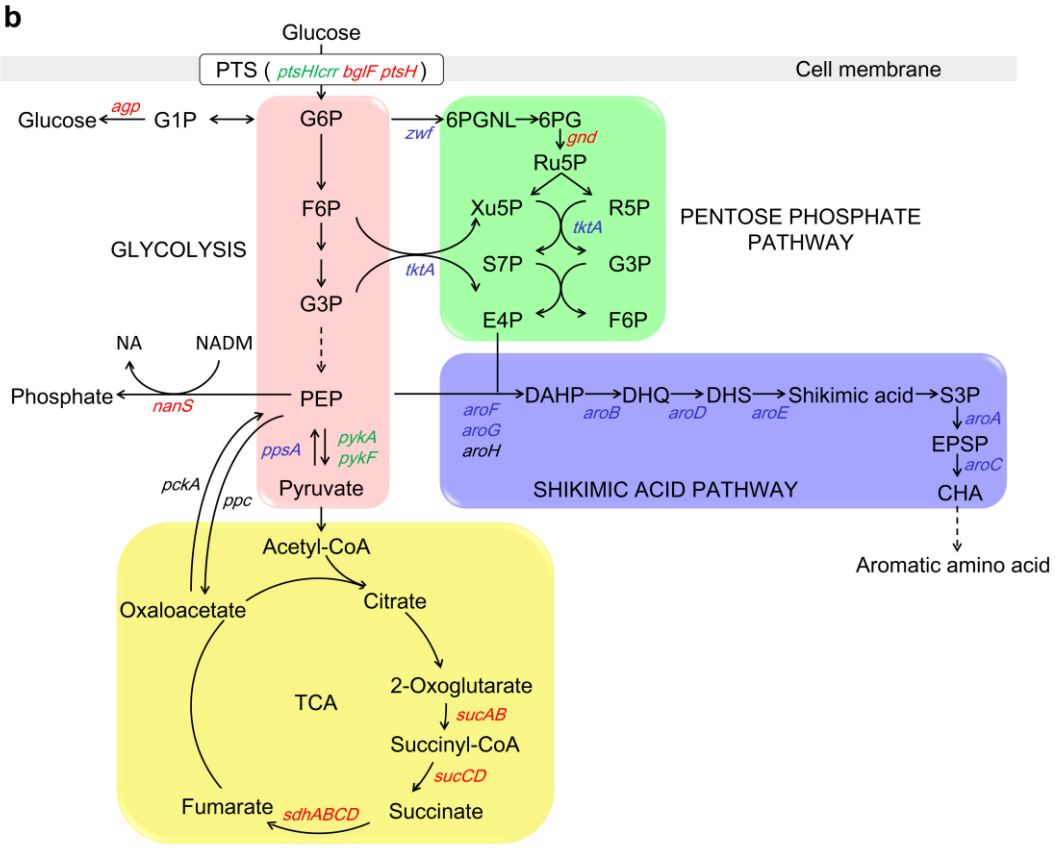
b
Glucose
PTS (ptsHIcrr bglF ptsH)
Cell membrane
Glucose
agp
G1P
G6P
zwf
6PGNL
6PG
gnd
Ru5P
F6P
Xu5P
R5P
tktA
GLYCOLYSIS
PENTOSE PHOSPHATE PATHWAY
S7P
G3P
E4P
F6P
NA
NADM
Phosphate
nanS
PEP
DAHP
DHQ
DHS
Shikimic acid
S3P
aroF
aroG
aroH
aroB
aroD
aroE
aroA
EPSP
aroC
CHA
ppsA
pykA
pykF
pckA
ppc
Pyruvate
SHIKIMIC ACID PATHWAY
Aromatic amino acid
Acetyl-CoA
Oxaloacetate
Citrate
TCA
2-Oxoglutarate
sucAB
Succinyl-CoA
sucCD
Fumarate
sdhABCD
Succinate

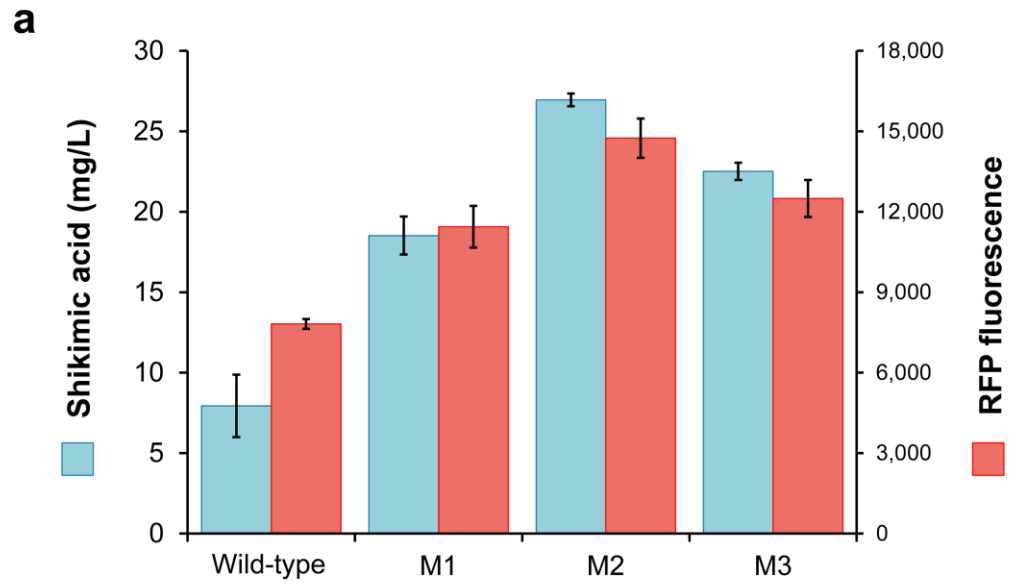
a
Shikimic acid (mg/L)
RFP fluorescence
30
25
20
15
10
5
0
18,000
15,000
12,000
9,000
6,000
3,000
0
Wild-type
M1
M2
M3

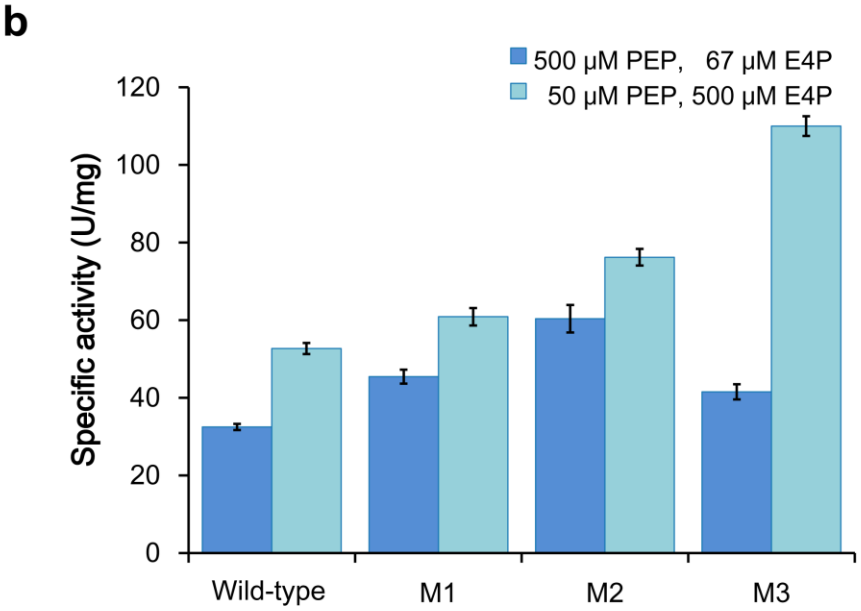
b
500 μM PEP, 67 μM E4P
50 μM PEP, 500 μM E4P
Specific activity (U/mg)
120
100
80
60
40
20
0
Wild-type
M1
M2
M3